Axions and X-ray polarimetry

Francesca Day

University of Cambridge

University of Sussex
November 2018

1801.10557: FD and S Krippendorf
In collaboration with S Krippendorf and F Marin

Outline

The Strong CP Problem

- The CP violating term $\mathcal{L} \supset \theta \frac{g^2}{32\pi^2} G^{\mu\nu} \tilde{G}_{\mu\nu}$ is allowed in the QCD Langrangian
- Null measurements of the neutron electric dipole moment constrain $\theta < 10^{-9}$
- Weak interactions transform θ: $\theta \to \theta + \arg \det M$.
- Need very fine tuned cancellations to explain observations.

The Vafa-Witten Theorem

"In parity-conserving vector-like theories such as QCD, parity conservation is not spontaneously broken."

Dynamical parity violating terms have zero vacuum expectation value.
(Vafa and Witten, 1984)

The Peccei-Quinn solution

- Promote θ to a dynamical variable - the QCD axion:
  $\mathcal{L} \supset \left(\theta + \frac{\xi a}{f_a}\right) \frac{g^2}{32\pi^2} G^{\mu\nu} \tilde{G}_{\mu\nu}$

- The Vafa-Witten theorem guarantees that the *total* θ term is zero in the ground state.

- A potential is generated for the axion such that the total coefficient of $G^{\mu\nu} \tilde{G}_{\mu\nu}$ is zero.

The Peccei-Quinn solution

- The θ term arises from the $U(1)_A$ anomaly of QCD
- To make θ dynamical, we introduce an additional global chiral symmetry $U(1)_{PQ}$, which is spontaneously broken.
- The axion is the Goldstone boson of $U(1)_{PQ}$.
- The QCD chiral anomaly causes non-perturbative explicit breaking of $U(1)_{PQ}$, generating a potential for the axion:

$$V \sim -\cos(\theta + \frac{\xi a}{f_a})$$

Axions

- Axions arise in extensions of the Standard Model as pseudo-Goldstone bosons of $U(1)_A$ symmetries.
- A generic axion is an ultra-light pseudo-scalar SM singlet.
- We may choose the axion basis such that one is the QCD axion and the rest have no coupling to gluons.
- We explore the phenomenology of the dimension 5 $aF_{\mu\nu}\tilde{F}^{\mu\nu}$ coupling.
- Axions may be observed through their conversion to photons in a background magnetic field.

Axions

- Axions are theoretically well motivated, but their cosmological abundance and phenomenology depends on many unknown parameters.

- We remain agnostic as to axion cosmology, and seek to constrain the existence of the axion in particle physics.

Axions

$$\mathcal{L} = \frac{1}{2}\partial_\mu a \partial^\mu a - \frac{1}{2}m_a^2 a^2 + \frac{a}{M}\mathbf{E} \cdot \mathbf{B}$$

- $\mathcal{L} \supset \frac{a}{M}\mathbf{E} \cdot \mathbf{B}$ leads to axion-photon interconversion in the presence of a background magnetic field.
- Model axion-photon conversion with classical equation of motion from $\mathcal{L}$.
- Assume that the axion wavelength is much shorter than the scale over which its environment changes, allowing us to linearise the equations of motion.

Axion-photon conversion

$$\left(\omega + \begin{pmatrix} \Delta_\gamma & 0 & \Delta_{\gamma ax} \\ 0 & \Delta_\gamma & \Delta_{\gamma ay} \\ \Delta_{\gamma ax} & \Delta_{\gamma ay} & \Delta_a \end{pmatrix} - i\partial_z \right) \begin{pmatrix} \mid \gamma_x \rangle \\ \mid \gamma_y \rangle \\ \mid a \rangle \end{pmatrix} = 0$$

- $\Delta_\gamma = \frac{-\omega_{pl}^2}{2\omega}$
- Plasma frequency: $\omega_{pl} = \left(4\pi\alpha \frac{n_e}{m_e} \right)^{\frac{1}{2}}$
- $\Delta_a = \frac{-m_a^2}{\omega}$.
- Here we take $m_a = 0$. This is valid for $m_a \lesssim 10^{-12}\,\mathrm{eV}$.
- Mixing: $\Delta_{\gamma ai} = \frac{B_i}{2M}$

$$P_{a \to \gamma}(L) = \mid \langle 1, 0, 0 | f(L) \rangle \mid^2 + \mid \langle 0, 1, 0 | f(L) \rangle \mid^2$$

Single domain

$$\tan(2\theta) = 10.0 \times 10^{-3} \times \left(\frac{10^{-3}\,\text{cm}^{-3}}{n_e}\right)\left(\frac{B_\perp}{1\,\mu\text{G}}\right)\left(\frac{\omega}{3.5\,\text{keV}}\right)\left(\frac{10^{13}\,\text{GeV}}{M}\right)$$

$$\Delta = 0.015 \times \left(\frac{n_e}{10^{-3}\,\text{cm}^{-3}}\right)\left(\frac{3.5\,\text{keV}}{\omega}\right)\left(\frac{L}{1\,\text{kpc}}\right)$$

$$P(a \rightarrow \gamma) = \sin^2(2\theta)\sin^2\left(\frac{\Delta}{\cos 2\theta}\right)$$

Axion-photon conversion

- $P_{a \to \gamma} \propto \frac{B_\perp^2}{M^2}$ for $\frac{B_\perp^2}{M^2} \ll 1$
- $P_{a \to \gamma}$ increases with the field coherence length and the total extent of the field.
- High electron densities increase the effective photon mass, suppressing conversion.
- Astrophysical environments lead to the highest conversion probabilities.
- The conversion probability is pseudo-sinusoidal in $1/E$.

Limits
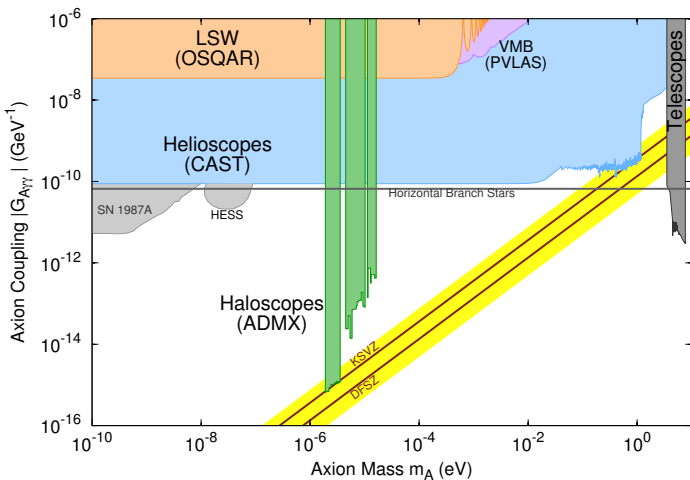
Reproduced from the Particle Data Group

Spectral Modulations

We search for axions by studying the X-ray spectra of point sources in or behind galaxy clusters.

Galaxy clusters

Photon-Axion Conversion

- Photon to axion conversion can lead to modulations in an initially pure photon spectrum, given by the photon survival probability $P_{\gamma \to \gamma}(E)$.
- At X-ray energies in galaxy clusters, $P_{\gamma \to \gamma}(E)$ is pseudo-sinusoidal in $\frac{1}{E}$.
- Axion induced oscillations in $P_{\gamma \to \gamma}(E)$ would be imprinted on the observed spectrum.
- We seek to constrain M by searching for such oscillations.

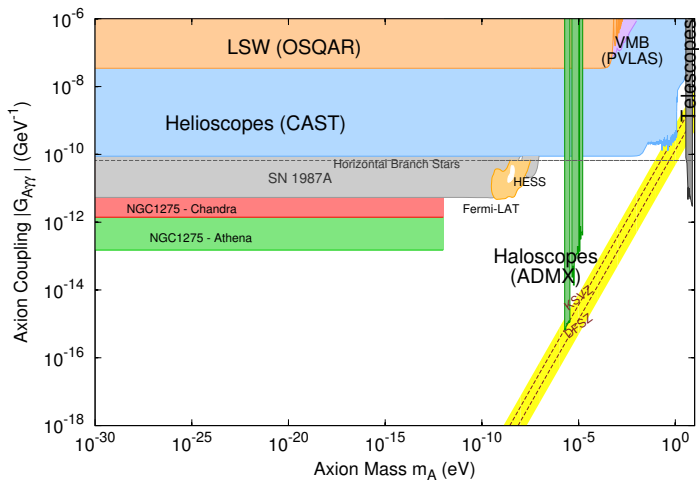# Photon survival probability
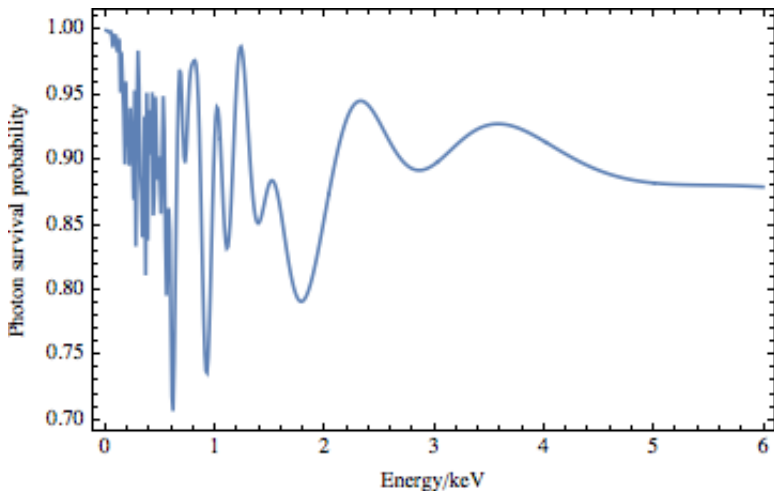
Example: NGC3862 in A1367
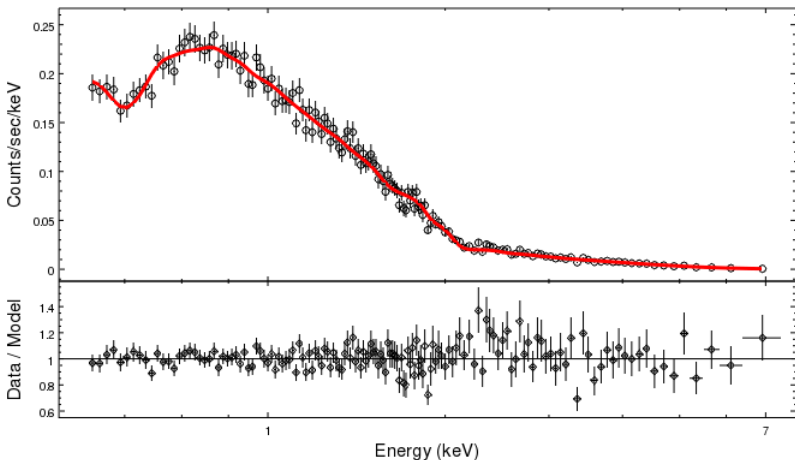
Bounds

The leading bounds are from NGC1275 in Perseus, 2E3140 in A1795 and M87 in Virgo: $M \gtrsim 7 \times 10^{11}$ GeV.

M Berg *et al* (1605.01043), J Conlon *et al*, (1704.05256), D Marsh *et al* (1703.07354)
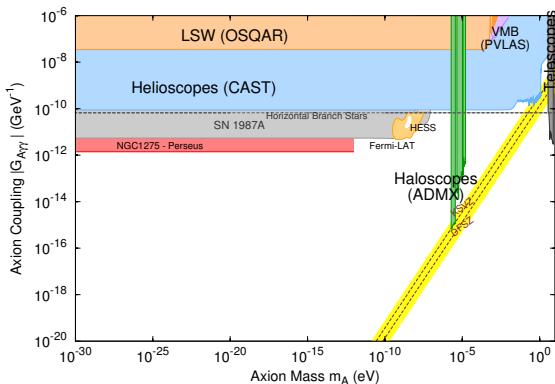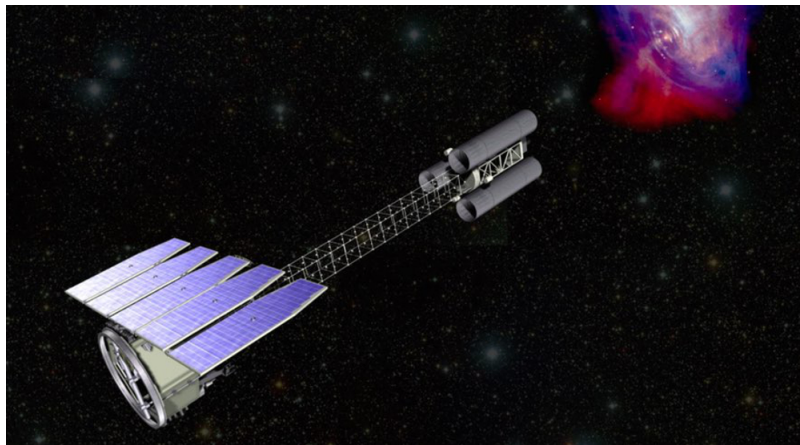
Projected bounds with Athena

J Conlon *et al*, (1707.00176)

Axion-photon conversion

$$\left(\omega + \begin{pmatrix} \Delta_\gamma & 0 & \Delta_{\gamma ax} \\ 0 & \Delta_\gamma & \Delta_{\gamma ay} \\ \Delta_{\gamma ax} & \Delta_{\gamma ay} & \Delta_a \end{pmatrix} - i\partial_z \right) \begin{pmatrix} \mid \gamma_x \rangle \\ \mid \gamma_y \rangle \\ \mid a \rangle \end{pmatrix} = 0$$

Only the photon polarization parallel to the external magnetic field participates in axion-photon conversion.

IXPE

Stokes parameters
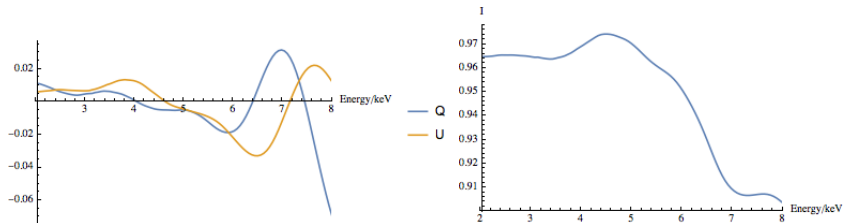
$$I = E_x^2 + E_y^2$$

$$Q = E_x^2 - E_y^2$$

$$U = 2\mathcal{R}e\left(E_x E_y^*\right)$$
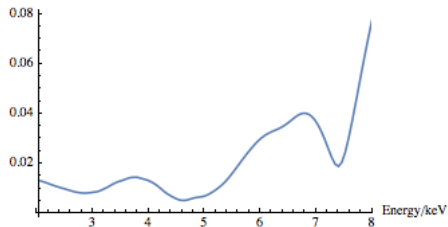
$$V = -2\mathcal{I}m\left(E_x E_y^*\right)$$

$$p_{\text{lin}} = \frac{\sqrt{Q^2 + U^2}}{I}$$

$$\psi = \frac{1}{2}\tan^{-1}\left(\frac{U}{Q}\right)$$

Polarimetry oscillations

Measurement

Basic implementation of detector errors from Kislat *et al* (1409.6214), using measured flux from NGC1275 and background from Perseus:

$$P(p_{\mathrm{lin}}, \psi | p_0, \psi_0) = \frac{\sqrt{I^2/W_2} p_{\mathrm{lin}} \mu^2}{2\pi\sigma} \times$$

$$\exp\left[-\frac{\mu^2}{4\sigma^2}\{p_0^2 + p_{\mathrm{lin}}^2 - 2p_0 p_{\mathrm{lin}} \cos(2(\psi_0 - \psi)) - \frac{p_0^2 p_{\mathrm{lin}}^2 \mu^2}{2} \sin^2(2(\psi - \psi_0))\}\right]$$

With

$$W_2 = (R_S + R_{BG})T(1 - f_{\mathrm{off}}) + R_{BG}\, Tf_{\mathrm{off}} \left(\frac{1 - f_{\mathrm{off}}}{f_{\mathrm{off}}}\right)^2, \qquad (2)$$

And

$$\sigma = \sqrt{\frac{W_2}{I^2}\left(1 - \frac{p_0^2 \mu^2}{2}\right)}. \qquad (3)$$

Polarimetry bounds

- Initially assume a featureless intrinsic AGN polarisation of 0%, 1% or 5%.
- Use the magnetic field experienced by photons from NGC1275 travelling through Perseus, marginalising over different field configurations
- Bin to IXPE's energy resolution
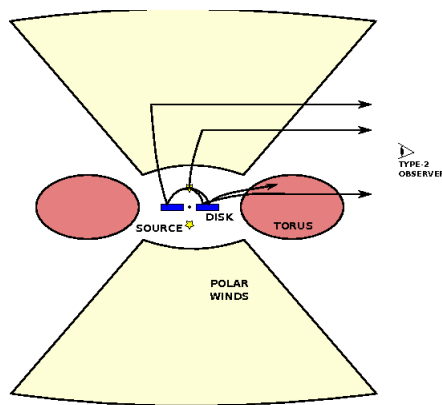- Compare a constant polarisation hypothesis with a constant source polarisation altered by axions

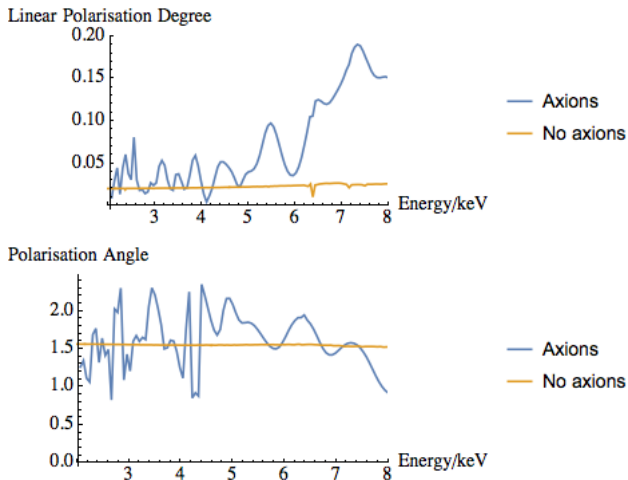# Polarimetry bounds
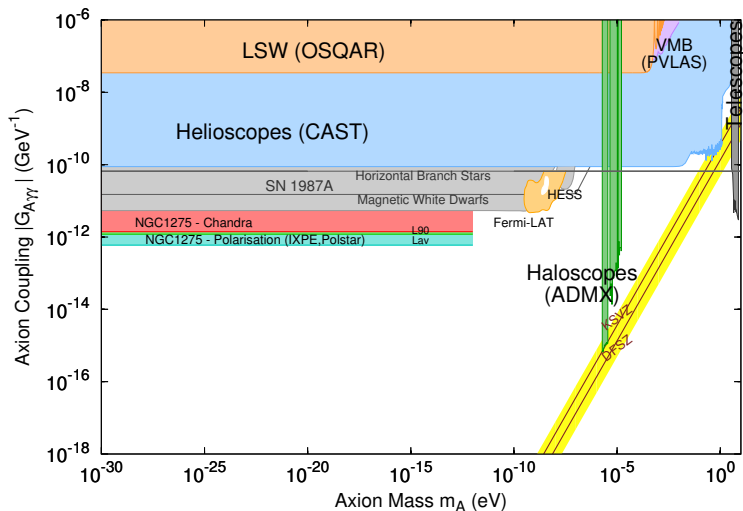
Next Steps

- Realistic source polarisation spectra

- Instrumental modelling
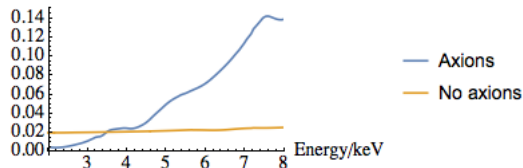
AGN

Reproduced from F Marin *et al*, 1709.03304
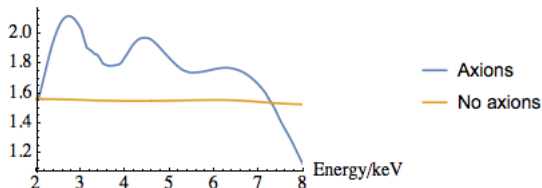
Type I AGN polarization

$$g_{a\gamma\gamma} = 10^{-12}\,\mathrm{GeV}^{-1}$$

Type I AGN polarization

$g_{a\gamma\gamma} = 10^{-12}\,\mathrm{GeV}^{-1}$

Type I AGN polarization

$$g_{a\gamma\gamma} = 3 \times 10^{-13}\,\mathrm{GeV}^{-1}$$

Type II AGN polarization
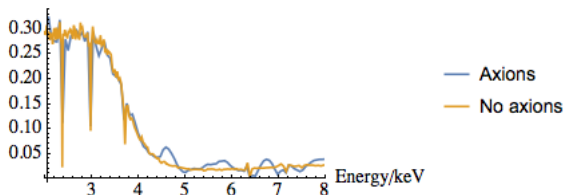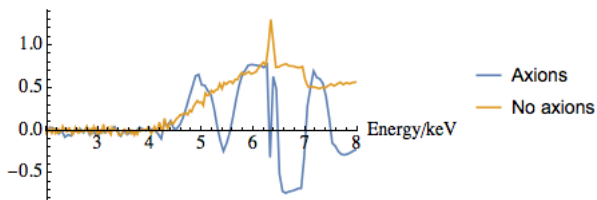
$$g_{a\gamma\gamma} = 10^{-12}\,\mathrm{GeV}^{-1}$$

Type II AGN polarization
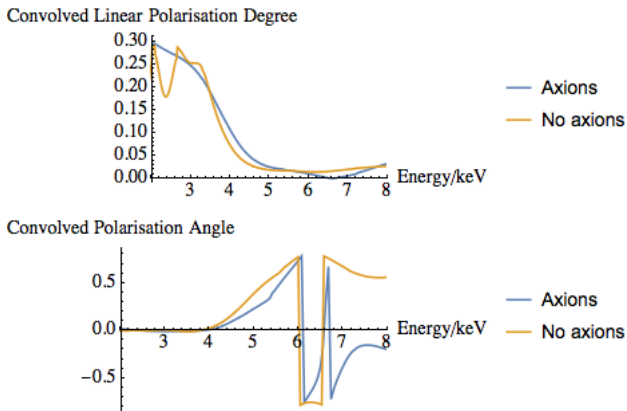
$g_{a\gamma\gamma} = 10^{-12}\,\mathrm{GeV}^{-1}$

Type I AGN Instrumental Modelling
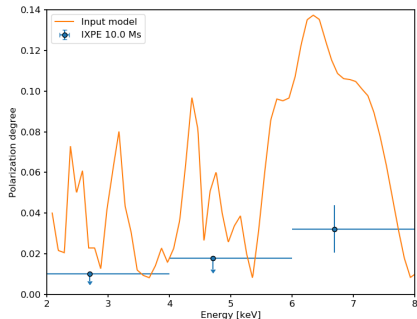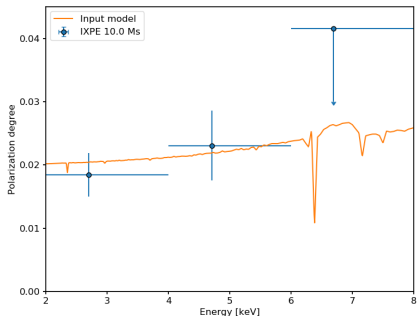
Work in progress

Future directions

- Type 2 targets

- Other telescopes: enhanced X-ray Timing and Polarimetry Mission

Conclusions

- The presence of axions may significantly alter the polarization spectra of AGN in or behind galaxy clusters.
- Axions can either decrease or increase measured polarization depending on bin size.
- Correlation between polarisation and flux anomalies may provide a smoking gun signal for axions.
- Axion effects may affect estimation of AGN parameters

Type I AGN Instrumental Modelling
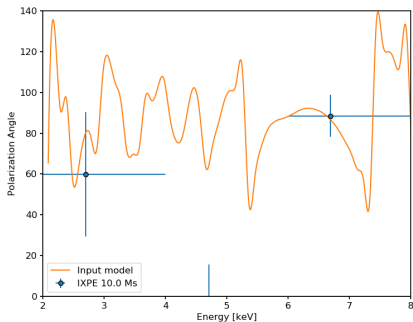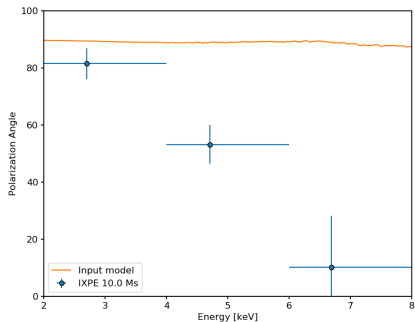
Bounds method 1

1. Randomly generate 1000 different magnetic field realisations $\mathbf{B}_i$ for the line of sight to NGC1275.

2. For each $\mathbf{B}_i$, generate the ALP induced linear polarisation $p_0^i(E)$ and polarisation angle $\psi_0^i(E)$ spectra, by numerically propagating the initial photon vector through the cluster.

3. From each $\{p_0^i(E), \psi_0^i(E)\}$ pair, generate 10 fake data sets.

4. Fit the no ALP constant model to each of the resulting 10,000 fake data sets, and find the corresponding likelihoods $\{L_{ga\gamma\gamma}^i\}$.

5. If fewer than 5% of the $\{L_{ga\gamma\gamma}^i\}$ are equal to or higher than $L_{\mathrm{noALP}}^{\mathrm{av}}$ (or L_{noALP}^{90} for the more pessimistic case), $g_{a\gamma\gamma}$ is excluded at the 95% confidence level.

Results 1

	0%	1%	5%
$L^{\mathrm{av}}_{\mathrm{noALP}}$	$1.2 \times 10^{-12}\,\mathrm{GeV}^{-1}$	$1.2 \times 10^{-12}\,\mathrm{GeV}^{-1}$	$6 \times 10^{-13}\,\mathrm{GeV}^{-1}$
L^{90}_{noALP}	$1.4 \times 10^{-12}\,\mathrm{GeV}^{-1}$	$1.3 \times 10^{-12}\,\mathrm{GeV}^{-1}$	$1.2 \times 10^{-12}\,\mathrm{GeV}^{-}$

Table: Projected upper limits on $g_{a\gamma\gamma}$ with IXPE. The columns correspond to different intrinsic polarisations of the AGN. The rows correspond to whether the average or 90th percentile likelihood value is used to characterize how well the no ALP model fits the simulated data.

Bounds method 2

- Follow *Fermi-LAT* (1603.06978)
- For each intrinsic source polarisation, simulate 1000 data sets $\{D_i\}$ with no ALPs present.
- Simulate transfer matrices for each value of g considered and for 100 different magnetic field configurations $\{B_j\}$.
- For each transfer matrix, find the final spectrum including ALPs for a range of different values for the intrinsic source polarisation degree $p_{\text{lin}}^{\text{source}}$ and angle ψ^{source}. We take $p_{\text{lin}}^{\text{source}} = 0 - 10\%$ in steps of 0.1% and $\psi^{\text{source}} = 0 - \pi$ in steps of $\frac{\pi}{100}$, and we use an interpolating function derived from this data for the maximisation procedure later on.

Bounds method 2

- We now fit the spectra with ALPs generated in the previous step to the fake data generated without ALPs. For each set (g, B_j, D_i) we find the values of $p_{\mathrm{lin}}^{\mathrm{source}}$ and ψ^{source} that maximize the likelihood
$L(g, B_j, p_{\mathrm{lin}}^{\mathrm{source}}, \psi^{\mathrm{source}} | D_i) = \prod_{\mathrm{bins}} L_k(g, B_j, p_{\mathrm{lin}}^{\mathrm{source}}, \psi^{\mathrm{source}} | D_i)$. In each bin k, L_k is the probability of measuring the p_{lin} and ψ values given by D_i, given that the true values are those predicted by an ALP model with parameters $(g, B_j, p_{\mathrm{lin}}^{\mathrm{source}}, \psi^{\mathrm{source}})$. These are calculated from Equation (1). We thus obtain a set of maximised likelihoods $L(g, B_j | D_i)$.

Bounds method 2

- For each value of g and each D_i, sort the $L(g, B_j | D_i)$ obtained from different magnetic fields, and select the 95th quantile L value, and the corresponding magnetic field. We thus obtain a set of likelihoods $L(g | D_i)$.
- For each D_i, find the value of g, $\hat{g}$ that leads to the maximum $L(g | D_i)$.
- We first consider the discovery potential of the data—i.e., the possibility of excluding a null hypothesis of no ALPs. For each D_i, we construct a test statistic $TS_i = -2\ln\left(\frac{L(g=0|D_i)}{L(g=\hat{g}|D_i)}\right)$.

Bounds method 2

- We have hence found the distribution of TS under a null hypothesis of no ALPs. We find the threshold TS value TS_{thresh} such that 95% of the TS_i are lower than TS_{thresh}. This value can be used to demonstrate our discovery potential for ALPs, by finding the TS for some of our fake data with ALPs included. We note that this test statistic does not obey Wilk's theorem as our hypotheses are not nested.

- We now turn to excluding values of g. Our null hypothesis is now that ALPs exist with some coupling g, and the alternative hypothesis H_1 is that $g \leq \hat{g}$. H_1 obviously includes the case where ALPs do not exist, but excluding ALPs with $g \leq \hat{g}$ should not be possible. Our test statistic for each g is now
$$\lambda(g, D_i) = -2\ln\left(\frac{L(g|D_i)}{L(\hat{g}|D_i)}\right).$$

Bounds Method 2

- We take the median value of $\lambda(g, D_i)$ over the D_i to represent that g. So we now have simply $\lambda(g)$ for our test statistic.
- We now need the null distribution of $\lambda(g)$ under the hypothesis that ALPs exist with coupling g. We assume that $\lambda(g)$ and the test statistic for a null hypothesis of no ALPs, TS above, have the same distribution, and therefore $\lambda(g)_{\mathrm{thresh}} = TS_{\mathrm{thresh}}$. We therefore exclude a value of g if $\lambda(g) > TS_{\mathrm{thresh}}$.

Results 2

	0%	1%	5%
$L_{\mathrm{noALP}}^{\mathrm{av}}$	$6 \times 10^{-13}\,\mathrm{GeV}^{-1}$	$9 \times 10^{-13}\,\mathrm{GeV}^{-1}$	$1.3 \times 10^{-12}\,\mathrm{GeV}^{-1}$

Table: Projected upper limits on $g_{a\gamma\gamma}$ with IXPE using the likelihood ratio method. The columns correspond to different intrinsic polarisations of the AGN.